JOURNAL OF SOLID STATE CHEMISTRY 83, 121–131 (1989)

Oxygen Vacancy Distribution in 6HBaFeO$_{3-y}$ ($0.20 \leq y \leq 0.35$)

M. PARRAS, M. VALLET-REGI, AND J. M. GONZÁLEZ-CALBET*

Departamento de Química Inorgánica, Facultad de Ciencias Químicas, Universidad Complutense, 28040-Madrid, Spain

AND J. C. GRENIER

Laboratoire de Chimie du Solide du CNRS, 33405 Talence-Cedex, France

Received March 10, 1989; in revised form July 19, 1989

An electron diffraction and microscopy study in the BaFeO$_{3-y}$ ($0.20 \leq y \leq 0.35$) system has been performed. For $0.25 \leq y \leq y$ 0.35 values, a phase of average composition BaFeO$_{2.75}$ intergrows, in a disordered way, with a cubic phase of composition close to BaFeO$_{2.50}$. For $0.20 \leq y \leq 0.25$ only a single 6H-type structure is observed. On the basis of these results and of a previous Mössbauer resonance study, several models of vacancy ordering are discussed.

Introduction

AMO_3 perovskites are usually described as a stacking sequence of AO_3 layers, M cations occupying a fraction of the octahedral holes. If the packing is cubic, a cubic perovskite is obtained, only three layers being necessary to describe the unit cell following a **ccc** sequence. For a hexagonal close packing, the $BaNiO_3$ structural type is obtained (*1*), only two layers being necessary to complete the unit cell (**hhh** sequence). Between both terms, several phases can be described (*2, 3*). Thus, the 6H structural type, characteristic of $BaTiO_3$ (*4*), is formed by a sequence **hcchcc** of AO_3 layers, i.e., two octahedra-sharing faces linked by octahedra-sharing corners.

In the BaFeO$_{3-y}$ system, the 6H-type is, as previously reported (*5, 6*), stable along a wide composition range. We have observed that, according to the method of preparation, materials between BaFeO$_{2.80}$ and BaFeO$_{2.65}$ present this structural type, all their powder X-ray diffraction data being similar to that of $BaTiO_3$.

We describe in this paper a study of the BaFeO$_{3-y}$ system by electron diffraction and electron microscopy which allows us to establish the relationship between the 6H structural type and the AMO_3 cubic perovskite. These results and those obtained by Mössbauer spectroscopy (*7*) lead us to propose several models for describing the vacancy accommodation as a function of the coordination of Fe atoms.

Experimental

Samples were prepared either by solid state reaction from BaO_2 and α-Fe_2O_3 or from the decomposition of a solution of barium and iron nitrate solution (*8*). In both

* To whom correspondence should be addressed.

0022-4596/89 $3.00

cases, the starting materials were heated, into open gold crucibles, at 890°C, resulting in a material with composition $BaFeO_{2.56}$. Then, several annealing procedures at $P_{O_2} = 0.2$ atm were performed, and the obtained materials are listed in Table I.

The chemical composition has been determined by measuring the iron oxidation state with a $K_2Cr_2O_7$ solution after dissolving the sample in 3*N* HCl with an excess of Mohr's salt.

Electron diffraction and microscopy have been performed on a JEOL 200 CX electron microscope, fitted with a double tilting goniometer stage, kindly lent to us by the INPG (Saint Martin d'Heres, France).

Results and Discussion

Figure 1 shows the electron diffraction pattern of $BaFeO_{2.75}$ along the $[010]_h$ zone axis which is parallel to the $[01\bar{1}]_c$ projection of the cubic perovskite sublattice. The electron diffraction pattern of the same sample corresponding to the $[001]_h//[1\bar{1}\bar{1}]_c$ zone axis is shown in Fig. 2 (subindexes h and c refer to hexagonal and cubic type unit cells, respectively). A sixfold superlattice along the $[1\bar{1}\,\bar{1}]_c^*$ and two threefold superlattices along the $[211]_c^*$ and $[12\bar{1}]_c^*$ are seen. From these results, the following relationship between the pseudocubic reciprocal subcell and the 6H hexagonal type reciprocal cell can be established:

$$a_h^* = 1/3[211]_c^*,$$
$$b_h^* = 1/3[12\bar{1}]_c^*,$$
$$c_h^* = 1/6[1\bar{1}\bar{1}]_c^*,$$

$$\begin{bmatrix} a \\ b \\ c \end{bmatrix}_h^* = \begin{bmatrix} 2/3 & 1/3 & 1/3 \\ 1/3 & 2/3 & \bar{1}/3 \\ 1/6 & \bar{1}/6 & \bar{1}/6 \end{bmatrix} \begin{bmatrix} a \\ b \\ c \end{bmatrix}_c^* \quad (1)$$

$$\mathbf{M}$$

As is well known, if $[a]_h^* = \mathbf{M}[a]_c^*$, the relationship between both direct cells is ex-

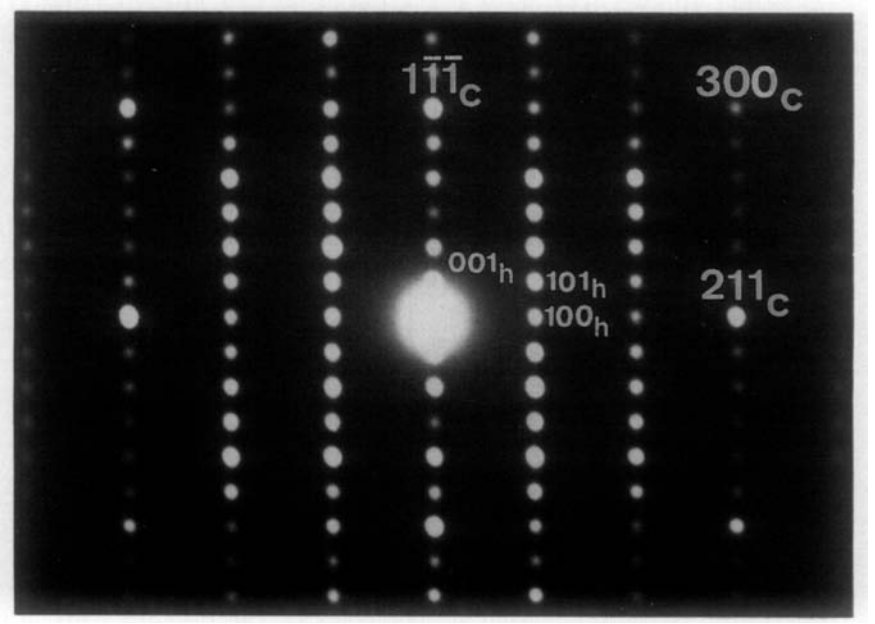

FIG. 1. Electron diffraction pattern of $BaFeO_{2.75}$ along the $[010]_h//[01\bar{1}]_c$ zone axis.

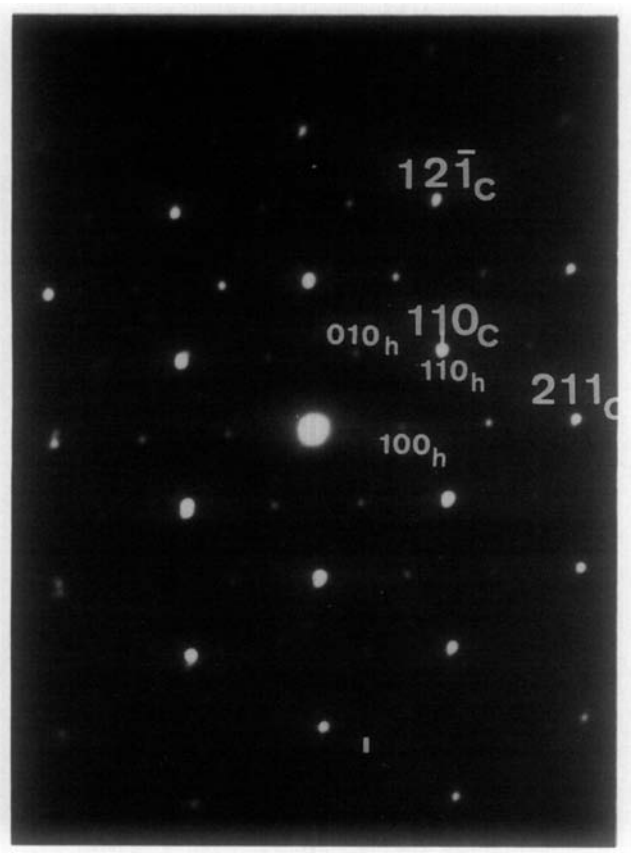

FIG. 2. Electron diffraction pattern of $BaFeO_{2.75}$ corresponding to the $[001]_h//[1\bar{1}\bar{1}]_c$ zone axis.

pressed by $[a]_h = ([\mathbf{M}]^{-1})^t[a]_c$, which according to Eq. (1), is

$$\begin{bmatrix} a \\ b \\ c \end{bmatrix}_h = \begin{bmatrix} 1 & 0 & 1 \\ 0 & 1 & \bar{1} \\ 2 & \bar{2} & \bar{2} \end{bmatrix} \begin{bmatrix} a \\ b \\ c \end{bmatrix}_c . \qquad (2)$$

From these results a relationship between both cubic and hexagonal structural parameters can be obtained:

$$\begin{aligned} \bar{a}_h &= \bar{a}_c + \bar{c}_c; & a_h &= \sqrt{2}a_c \\ \bar{b}_h &= \bar{b}_c - \bar{c}_c; & b_h &= \sqrt{2}a_c \\ \bar{c}_h &= 2\bar{a}_c - 2\bar{b}_c - 2\bar{c}_c; & c_h &= 2\sqrt{3}a_c. \end{aligned} \qquad (3)$$

Figure 3a schematizes the relationship between the cubic and the hexagonal reciprocal cells while Fig. 3b shows such a relation between both direct cells.

Figure 4a shows the hexagonal cell structural model of the hexagonal cell along $[110]_h$. It can be observed that, following

TABLE I

OBTAINED MATERIALS IN THE $BaFeO_{3-y}$ ($0.20 < y < 0.35$) SYSTEM

T(°C)	t(hr)	Fe^{4+}(%)	Composition
650	48	56	$BaFeO_{2.79}$
680	48	50	$BaFeO_{2.75}$
700	48	46	$BaFeO_{2.73}$
750	48	38	$BaFeO_{2.69}$
780	48	28	$BaFeO_{2.64}$

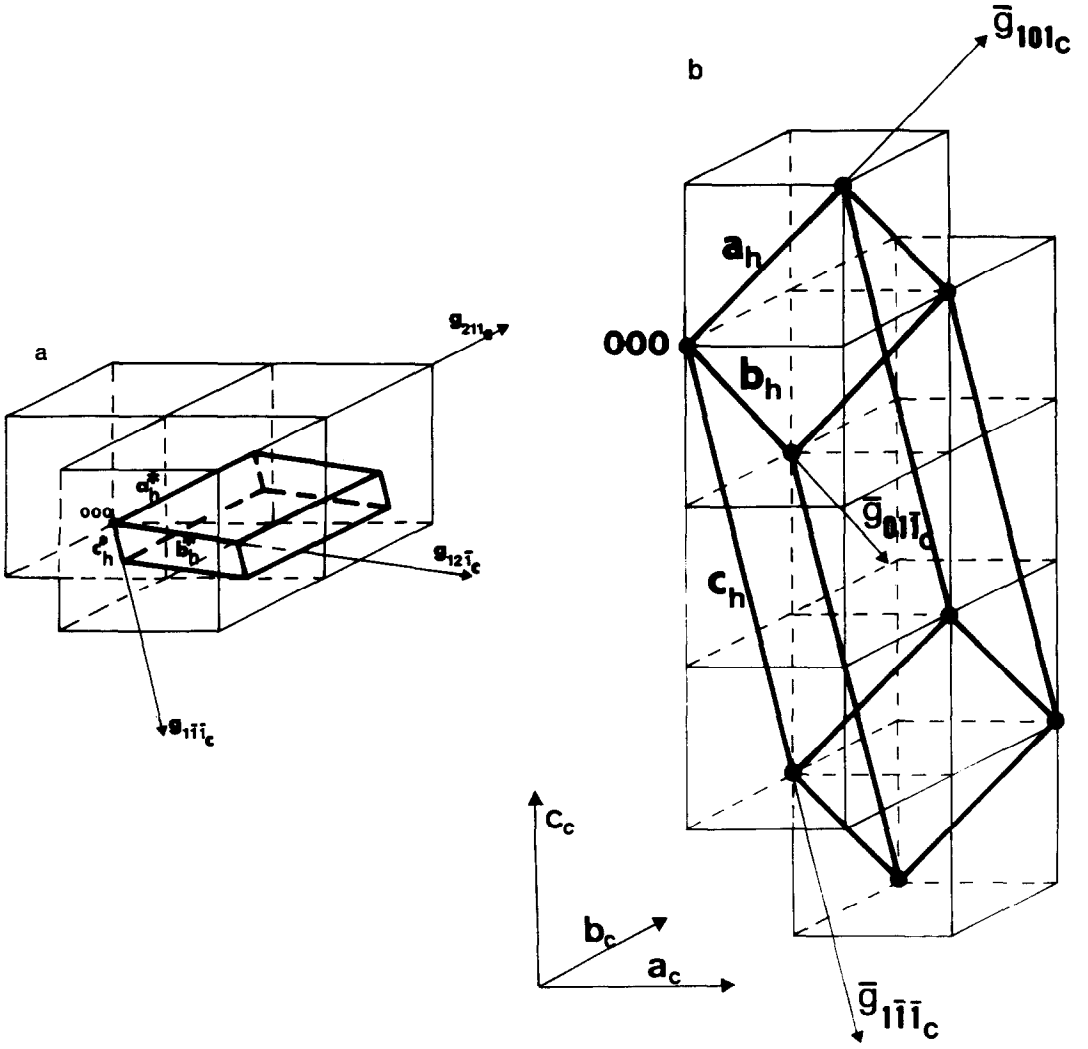

FIG. 3. (a) Schematic representation of the 6H-type reciprocal lattice showing the relative orientation with respect to the cubic perovskite reciprocal cell. (b) Schematic representation of both hexagonal and cubic direct cells.

the **c** axis, couples of octahedra-sharing faces, tilted 180° with respect to the next octahedra couple, are separated by a cubic layer, i.e., an octahedron-sharing vertex. This sequence justifies the sixfold superlattice along this direction.

On the other hand, a threefold superlattice with respect to the cubic subcell appears along both $(211)_c//(100)_h$ and $(12\bar{1})_c//(010)_h$ due to the relative disposition of the octahedra, as schematically represented in Fig. 4b.

As we have previously mentioned, powder X-ray diffraction patterns of materials in the $BaFeO_{2.80}$–$BaFeO_{2.65}$ composition range were either similar or identical to that shown by $BaTiO_3$. Even the electron diffraction patterns of this stoichiometric compound are identical to those observed for $BaFeO_{2.75}$ (8.3% of the vacancies). Fig-

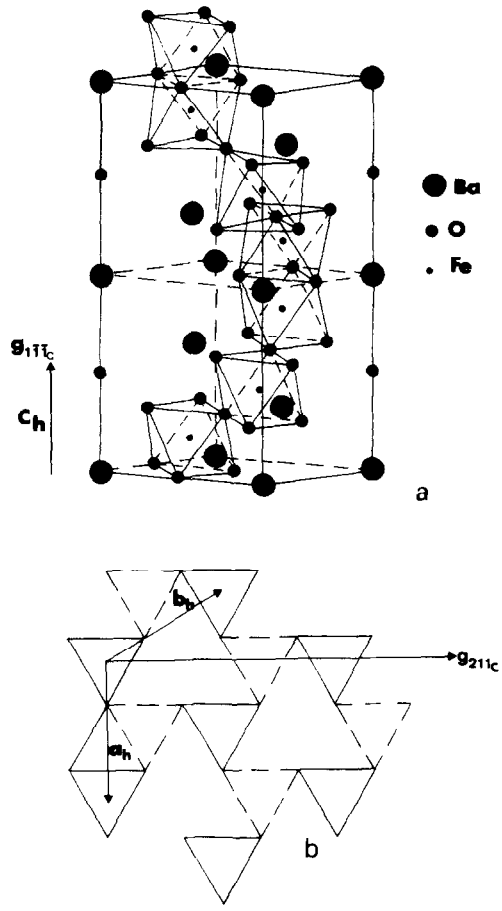

FIG. 4. (a) Structural model of the 6H-type phase. (b) Schematic representation of the (*ab*) plane corresponding to the 6H structural type.

ures 5a and 5b show the electron diffraction patterns along $[010]_h$ and corresponding micrographs for $BaFeO_{2.75}$ and $BaTiO_3$, respectively.

However, if the Fe^{4+} amount decreases, some differences appear. Figure 6 shows the structure image corresponding to Ba $FeO_{2.70}$ and $[010]_h$. It can be observed that $BaFeO_{2.75}$ is apparently ordered, while Ba $FeO_{2.70}$ shows stacking faults along the c_h axis which are marked by an arrow. In these areas, it can be observed that crystallographic planes separated by 4 Å intersect at 45° the $(001)_h$ planes which can be attributed to a cubic sublattice. Both samples have been annealed following an identical path (*8*), suggesting that the differences observed can be related to their different composition. If this is true, and if we assume that the composition in the ordered phase is close to $BaFeO_{2.75}$, the composition in the arrowed domains must show a lower oxygen content, leading to a composition of $BaFeO_{2.70}$. These results seem to indicate that if the Fe^{4+} amount decreases, the AO_3 packing changes from hexagonal to cubic, since the Goldschmidt factor decreases (*9*) due to the increase of the atomic radium of *M* cations.

In a previous study (*7*), the interpretation of the Mössbauer spectrum obtained for a composition close to $BaFeO_{2.75}$ (*7*) led to the following ideal cationic distribution:

—50% of high spin Fe^{4+} in [V] coordination;
—50% of Fe^{3+} in [VI] coordination;
—No tetrahedral coordination was detected.

The ensemble of results obtained by electron diffraction and microscopy and Mössbauer spectroscopy allow us to propose the following conclusions:

—The phase without extended defects shows a chemical composition close to Ba $FeO_{2.75}$ with 50% Fe^{4+} in [V] coordination and 50% Fe^{3+} in octahedral sites.
—No differences are observed by electron diffraction between $BaFeO_{2.75}$ and Ba TiO_3, suggesting that vacancies either are at random or are ordered in such a manner that a 6H-type cell is maintained.

In order to keep a 6H-type unit cell for the $BaFeO_{2.75}$ composition without the formation of a superlattice due to oxygen vacancies, two solutions can be imagined:

(1) The first solution has different oxygen compositions in adjacent layers:

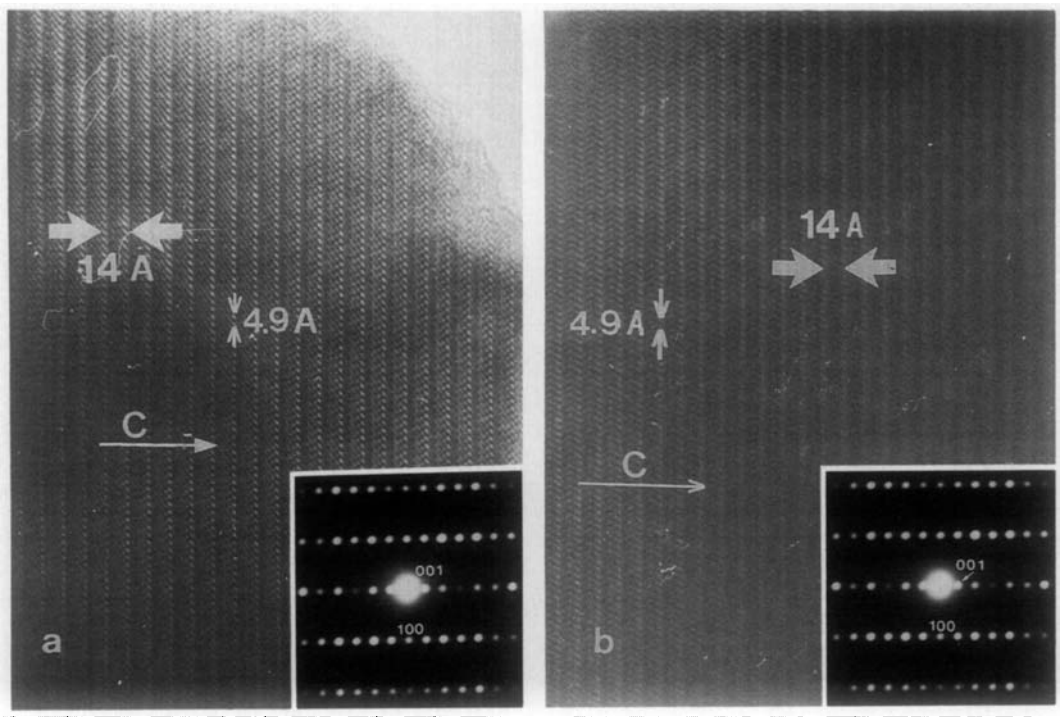

FIG. 5. (a) Electron micrograph and corresponding electron diffraction pattern of $BaFeO_{2.75}$ along the $[010]_h$ zone axis. (b) Same as (a) but for $BaTiO_3$.

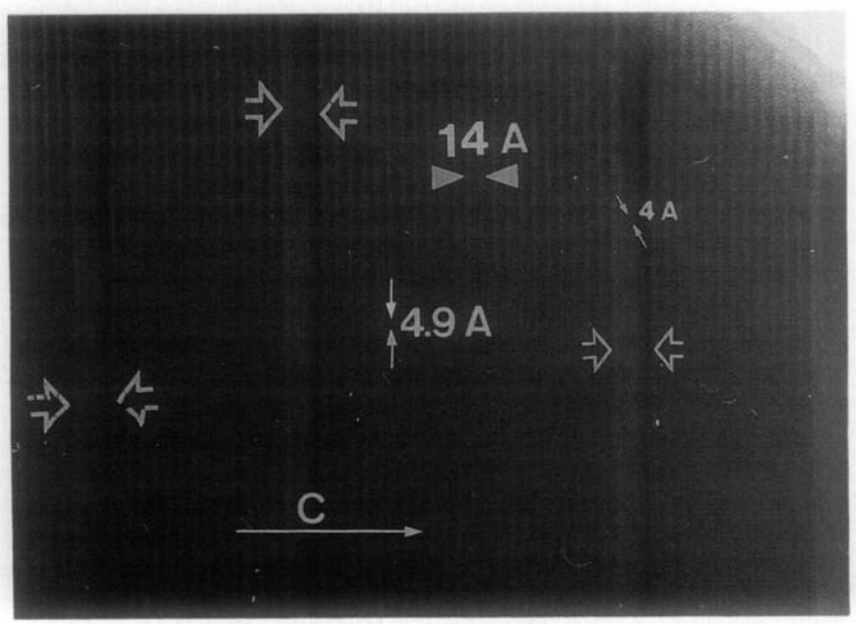

FIG. 6. Electron microscopic image of $BaFeO_{2.70}$ showing a disordered intergrowth of $BaFeO_{2.75}$ and a cubic phase.

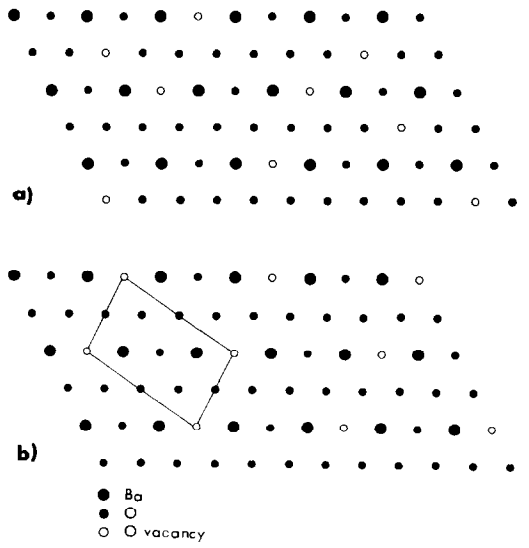

FIG. 7. Schematic representation of an $AO_{2.50}$ layer showing: (a) anionic distribution at random, (b) ordering of the oxygen vacancies. The resulting orthorhombic cell is outlined.

h, AO_{3-x}
c, $AO_{2.5+x}$
c, AO_{3-x}
h, $AO_{2.5+x}$
c, AO_{3-x}
c, $AO_{2.5+x}$
h, AO_{3-x}.

This leads to several solutions ($0 \leq x \leq 0.25$), assuming in every case that a disorder of the vacancies in the (*ab*) plane occurs. The only restriction is that the partial ordering cannot result in the formation of tetrahedra.

Among these possibilities, it is interesting to consider more carefully one particular case. When $x = 0$, the anionic distribution in the AO_3 layers is as follows:

h, AO_3
c, $AO_{2.5}$
c, AO_3
h, $AO_{2.5}$
c, AO_3
c, $AO_{2.5}$
h, AO_3.

In this case, we could suppose that oxygen vacancies are either distributed at random in the $AO_{2.5}$ layers, as shown in Fig. 7a, or ordered, as schematized in Fig. 7b, inducing an orthorhombic superlattice in the (*ab*) hexagonal plane. This ordering leads to a unit cell with two parameters that are parallel to the **b** and **c** hexagonal axes and the third one, perpendicular to them, would follow the $[210]_h$ direction.

If we represent schematically the patterns of Figs. 1 and 2, all the reflections can be indexed on the basis of an orthorhombic cell (Figs. 8a and b) in such a way that if we consider the extinctions shown in both figures, no differences can be detected between the patterns of this new phase and of that corresponding to the previous 6H-type cell. Besides, only reflections (*hkl*) when $(h + k) = 2n$ appear in the electron diffraction pattern corresponding to the $[011]_h//[011]_o$ zone axis (Fig. 9a), which is schematized in Fig. 9b (subindex o refers to the orthorhombic cell). According to these extinctions, *C*222, *Cmmm*, and *Cmm*2 space groups are possible (*10*).

From these results, it follows that the geometric relationship between the orthorhombic and hexagonal reciprocal cells (see Fig. 10a) is given by the expression

$$\begin{bmatrix} a \\ b \\ c \end{bmatrix}^*_o = \begin{bmatrix} 1/2 & 0 & 0 \\ \bar{1}/2 & 0 & 0 \\ 0 & 0 & 1 \end{bmatrix} \begin{bmatrix} a \\ b \\ c \end{bmatrix}^*_h . \qquad (4)$$

And the corresponding relationship between both direct cells (Fig. 10b) is

$$\begin{bmatrix} a \\ b \\ c \end{bmatrix}_o = \begin{bmatrix} 2 & 1 & 0 \\ 0 & 1 & 0 \\ 0 & 0 & 1 \end{bmatrix} \begin{bmatrix} a \\ b \\ c \end{bmatrix}_h . \qquad (5)$$

Then, the structural parameters are related by means of the expressions

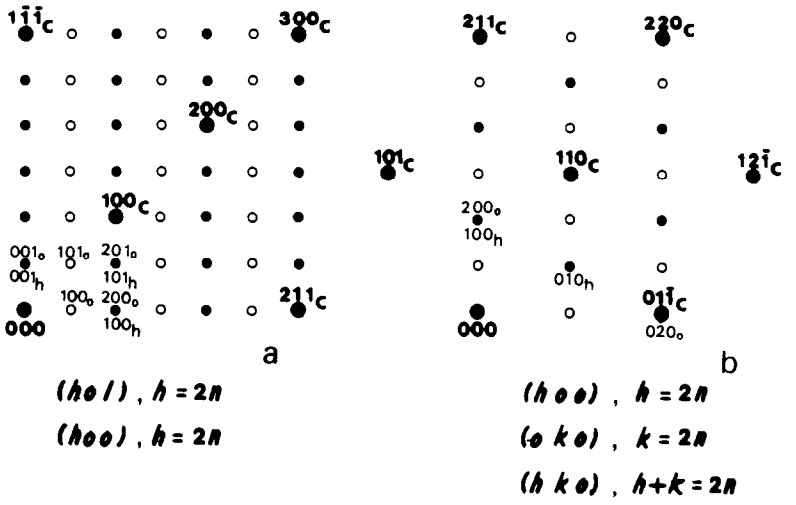

FIG. 8. Schematic representation of the electron diffraction patterns shown in Figs. 1 and 2. Void dots correspond to systematic extinctions: (a) zone axis: $[010]_h//[010]_o$. (b) Zone axis: $[001]_h//[001]_o$.

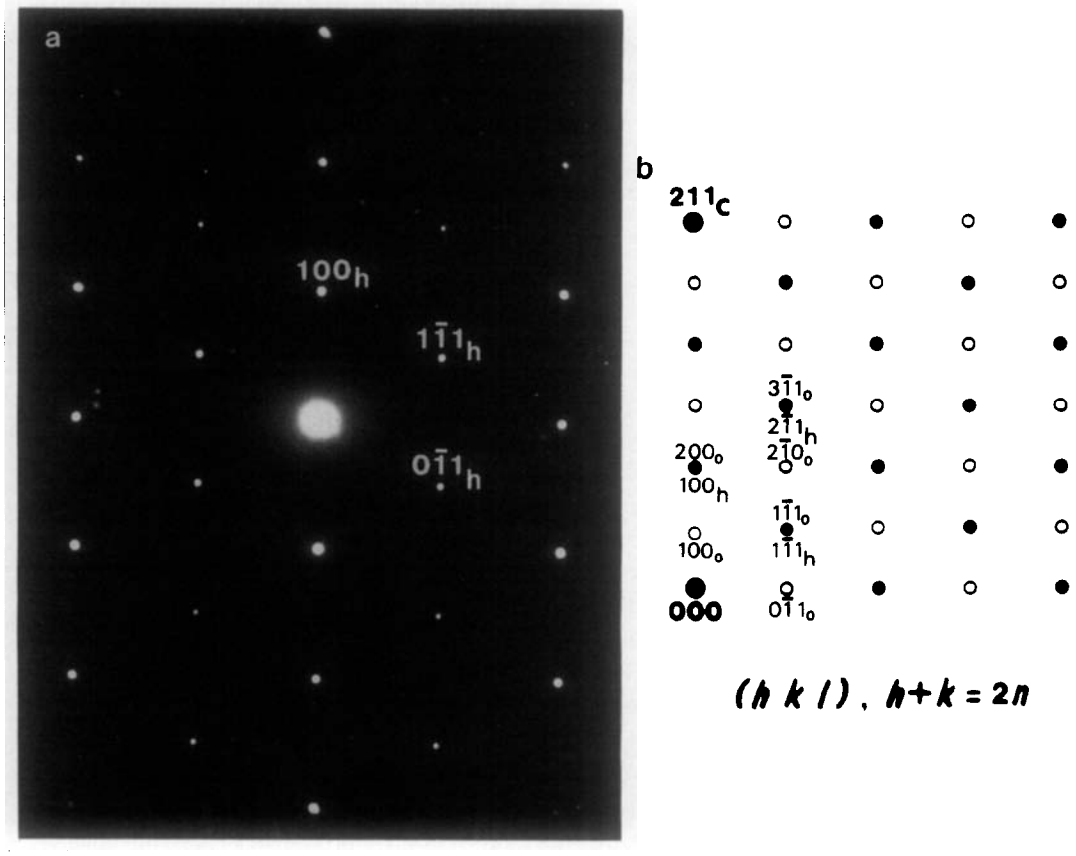

FIG. 9. (a) Electron diffraction pattern of $BaFeO_{2.75}$ along $[011]_h//[011]_o$. (b) Schematic representation of the above pattern showing the extinctions for the orthorhombic cell.

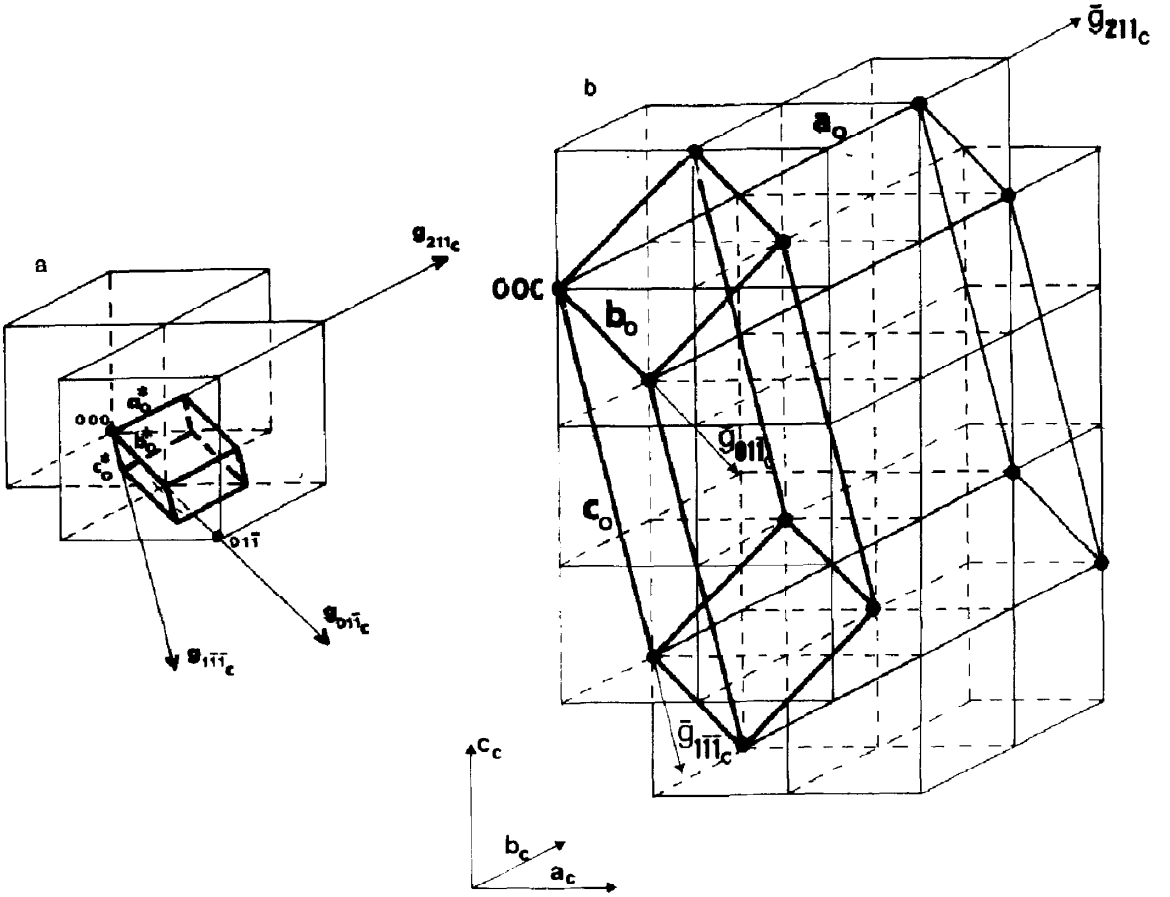

FIG. 10. (a) Schematic representation of the relationship between the orthorhombic and pseudocubic reciprocal lattices. (b) Same as (a) but for the direct cells.

$$\begin{aligned} \bar{a}_o &= 2\bar{a}_h + \bar{b}_h; & a_o &= \sqrt{3}a_h \\ \bar{b}_o &= \bar{b}_h; & b_o &= b_h \\ \bar{c}_o &= \bar{c}_h; & c_o &= c_h. \end{aligned} \qquad (6)$$

(2) The second solution consists in considering that all **h** planes (and, in the same way, all **c** planes) have the same composition. In order to obtain a $BaFeO_{2.75}$ average composition following the stacking sequence $(hcc)_2$, it is necessary to solve the equation

$$2AO_x + AO_y = A_3O_{8.25}, \qquad (7)$$

where x and y are the oxygen compositions of the **c** and **h** layers, respectively.

According to previous results (*11*), it can be assumed that the lower composition for a given layer is $AO_{2.5}$. Thus, the possible values for x and y will be in the $2.5 \leq x, y \leq 3.0$ range.

Among several solutions, we emphasize the following anionic distribution which was previously proposed by Jacobson (*11*) from neutron diffraction results:

h, $AO_{2.5}$
c, $AO_{2.875}$
c, $AO_{2.875}$
h, $AO_{2.5}$
c, $AO_{2.875}$
c, $AO_{2.875}$
h, $AO_{2.5}$.

The oxygen vacancy distribution was interpreted in terms of the formation of tetrahedra which were not observed in our samples by Mössbauer spectroscopy.

According to the composition and considering the X-ray and electron diffraction, electron microscopy, and Mössbauer spectroscopy results, the anion vacancies (4.16%) should be distributed at random along the **c** layers. On the other hand, the concentration of oxygen vacancies in the **h** layers (16.6%) could lead to some type of ordering. However, since tetrahedra are not observed by Mössbauer spectroscopy, vacancies in the **h** layers must also be disordered in such a way that IV coordination is avoided. According to this distribution, superstructure reflections are not observed in electron diffraction patterns.

Previous studies on nonstoichiometry in AMO_{3-y} perovskites have clearly shown that the vacancy ordering is a function of **y**. For instance, Komornicki *et al.* (*12*) hypothesized in perovskite-related ferrites that for values of **y** close to 0.15, oxygen vacancies were thought to be ordered along rows of various lengths in a statistical fashion, preserving the perovskite symmetry, these developing into vacancy rows of infinite length as **y** approach ca. 0.20. When **y** is ca. 0.25, the vacancy rows order into planes; and for still larger values of **y** the number of tetrahedral planes increases giving rise, as seen by electron diffraction and high resolution electron microscopy, to either disordered intergrowths (*13, 14*) or new ordered phases (*15, 16*).

This model seems to be satisfactory for perovskite-related ferrites when octahedral and tetrahedral layers alternate along one axis. There are, however, structurally analogous compounds with different transition metal cations, where no evidence of the occurrence of the various kinds of vacancy clusters envisaged by Komornicki *et al.* has been found. This is the case, for instance, of $CaMnO_{3-y}$ materials, where the existence of square-pyramidal coordination for Mn^{3+} (*17*) has been proved, and ordered structures in the $0 \leq y \leq 0.5$ range, even at **y** values close to 0, seem to exist (*18*).

In the $BaFeO_{3-y}$ system, the accommodation of the nonstoichiometry follows a model different from that proposed by Komornicki *et al.* (*12*), and even for **y** values higher than 0.25, no superstructure reflections, indicative of some kind of ordering with respect to the stoichiometric $BaTiO_3$ 6H-type compound, are seen. Thus, although Fe^{4+} in [V] coordination is detected, the structural feature governing the anionic distribution seems to be the presence of coordination polyhedra-sharing faces, since in the materials formed by geometric environments sharing corners, the high resolution lattice image contrast is easily used as a criterion to distinguish among the various possibilities of vacancy ordering even at low **y** values.

More studies on nonstoichiometric hexagonal perovskites are necessary to hypothesize about the kind of vacancy ordering as a function of **y**.

References

1. J. J. Lander, *Acta Crystallogr.* **4,** 148 (1951).
2. L. Katz and R. Ward, *Inorg. Chem.* **3**(2), 205 (1964).
3. T. Negas and R. S. Roth, *J. Solid State Chem.* **3,** 323 (1971).
4. R. D. Burbank and H. T. Evans, *Acta Crystallogr.* **1,** 330 (1948).
5. S. Mori, *J. Amer. Chem. Soc.* **49,** 600 (1965).
6. G. Gleitzer, M. Zanne, and C. Zeller, *C.R. Acad. Sci. Paris* **270,** 1496 (1970).
7. J. C. Grenier, L. Fournes, M. Pouchard, P. Hagenmuller, M. Parras, M. Vallet, and J. Calbet, *Z. Anorg. Allg. Chem.* (1989, in press).
8. J. C. Grenier, A. Wattiaux, M. Pouchard, P. Hagenmuller, M. Parras, M. Vallet-Regi, J. González-Calbet, and M. A. Alario, *J. Solid State Chem.* **80,** 6 (1989).
9. V. H. Goldschmidt "Geochem. Verteilungsgesetze der Elemente VII, VIII" (1927, 1928).
10. "International Tables for X-Ray Crystallography," Vol. A, Publishing Company (1987).

11. A. J. JACOBSON, *Acta Crystallogr. B* **32,** 1087 (1976).
12. S. KOMORNICKI, J. C. GRENIER, M. POUCHARD, AND P. HAGENMULLER, *Nouv. J. Chim.* **5,** 161 (1981).
13. J. M. GONZÁLEZ-CALBET, M. VALLET-REGI, M. ALARIO-FRANCO, AND J. C. GRENIER, *Mat. Res. Bull.* **18,** 285 (1983).
14. M. VALLET-REGI, J. M. GONZÁLEZ-CALBET, M. ALARIO-FRANCO, J. C. GRENIER, AND P. HAGENMULLER, *J. Solid State Chem.* **55,** 251 (1984).
15. J. C. GRENIER, J. DARRIET, M. POUCHARD, AND P. HAGENMULLER, *Mat. Res. Bull.* **11,** 1219 (1976).
16. J. M. GONZÁLEZ-CALBET AND M. VALLET-REGI, *J. Solid State Chem.* **68,** 266 (1987).
17. K. R. POEPPELMEIER, M. E. LEONOWICZ, AND J. M. LONGO, *J. Solid State Chem.* **44,** 89 (1982).
18. A. RELLER, J. M. THOMAS, D. A. JEFFERSON, AND M. K. UPPAL, *Proc. R. Soc. London Ser. A* **394,** 223 (1984).